First Report on *Butea monosperma* Flower Extract Based Nickel Nanoparticles Green Synthesis and Characterization

Ujwala S. Tayade[1], Amulrao U.Borse*[2], Jyotsna S. Meshram*[3]

[1]School of Chemical Sciences, Chemistry, University North Maharashtra University, Jalgaon, Maharashtra, India
[2]School of Chemical Sciences, Chemistry, University North Maharashtra University, Jalgaon, Maharashtra, India
[3]Department of Chemistry, Rashtrasant Tukadoji Maharaj Nagpur University, Nagpur, Maharashtra, India

ABSTRACT

Herein we study the *Butea monosperma* for the preparation of nickel nanoparticles. The plant extraction carried out in aqueous medium and screening for exact phytochemicals present in it. The nickel nanoparticles were prepared by one-step in simple, cheap and less time-consuming manner. The nickel nanoparticles are important for their semiconductor properties. We, therefore, study its optical properties by using taucs plot method. This also proves that confirmation of nanoparticles synthesized. The increase in band gap value indicates that decrease in particle size i.e. nanoparticle synthesis. The plant extract was used in various fields such as medicines, dyes, and pesticides. Here the report of plant extracts as a reducing agent in nanoparticle synthesis. The nanoparticles synthesis were confirmed by various characterizations techniques such as Ultraviolet -Visible spectrometer (UV), Fourier transform-Infrared spectrometer (FT-IR), X-ray diffraction (XRD), Scanning electron microscope (SEM) and calculating its band gap value which is 3.85 eV.

Keywords: Nickel Nanoparticles; *Butea monosperma*; Phytochemicals Screening; Semiconductor; Band Gap

I. INTRODUCTION
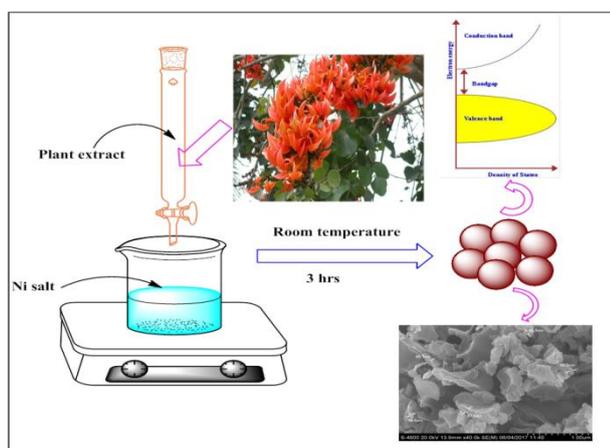
Figure 1. Graphical abstract of Nickel nanoparticles synthesis

In the nanotechnology, nickel nanoparticles have been received more attention due to their electrical, magnetic and catalytic properties [1]. The wide range of application in various fields including the fabrication of catalysis, electrochromic films, fuel cell electrodes and gas sensors, battery cathodes, pn-junctions, magnetic materials, photovoltaic devices, electrochemical supercapacitors, smart windows and dye-sensitized photocathodes [2]. Therefore, NiO became one of the most important transition metal oxides. However, most of these applications require particles with a small size and a narrow size distribution. With the volume effect, the quantum size effect and the surface effect, NiO nanoparticles were expected to possess many improved properties and even more attractive applications than those of bulk-sized NiO particles. The plant-mediated synthesis of nickel nanoparticles is having more importance over the conventional method. This requires number of chemicals, instruments for the methods like laser ablation, lithography, chemical reduction method, thermal decomposition [3-5], carbonyl method, sol-gel technique [6], microwave pyrolysis [7], solvothermal [8], anodic arc plasma [9], sonochemical [10], precipitation [11] and microemulsion [12].The green approach in nanomaterial's synthesis is superior to other synthetic methods because of cost-effectiveness, less optimization required and easy synthesis. Therefore, the

combination of biological principles (i.e., oxidation/ reduction) by microbial enzymes or plant phytochemicals with physical and chemical approaches results in the synthesis of nanoparticles (NPS) with desired functions [13-15]. NPS with an added advantage of stabilizing the formed NPS as plant secondary metabolites besides acting as synthetic agents also acts as a capping agent. Recently, NiO NPS were studied widely because of their electro catalysis, high chemical stability, super conductance characteristics, and electron transfer capability [16]. NiO is a p-type semiconductor metal oxide having a band gap ranging from 3.6 to 4.0 eV depending upon the nature of defects and their density. The bio-based method is important in case of nanomaterial synthesis some basic requirement should follow by them such as i] choice of proper solvent, ii] choice of an eco-friendly reducing agent and iii] choice of non-toxic stabilizing agent for NPS. Thus by choosing proper solvent, surfactant and reductant biosynthesis produces NPS with controlled morphology without producing any toxic environmental pollutant [17].The essential property of bio-synthesis is that they produce a non-toxic nanomaterial which is useful in biomedical and drug delivery system by removing toxic surfaces of nanoparticles.

In the present study, the *Butea monosperma* (*B.monosperma*) based nickel oxide nanoparticles were formed by the green approach. The phytochemicals present in the extract were useful for reduction as well as the capping of the metal precursor to form nanoparticles. Also, the solvent for extraction and preparation of nanoparticles is water that is more suitable for synthesis. We analyzed the phytochemicals present in it by standard protocol. The phytochemicals of *B.monosperma* are more soluble in water as compare to any other solvents. All aspects of green chemistry followed by nickel nanoparticles and show the special morphological property with optical properties shows the band gap value of 3.5 eV.

II. EXPERIMENTAL

Materials: Nickel nitrate hexahydrate (Ni NO_3.$6H_2O$) [Sigma Aldrich], Deionized water, *Butea monosperma* petals etc.

Method:

Preparation of plant extract:

The 1 gm. of *Butea monosperma* petals were washed and dried. Then the petals were crushed in mortar and piston. The crushed petals are mixed with 100 ml of deionized water and continue the reflux condensation for 2 hrs. After that plant extract were filtered through Whatman filter paper. The filtrate is used as plant extract for further uses it is stored at 4°C.

Phytochemical Screening:

Qualitative Analysis

Following standard protocols were used for qualitative analysis of samples to check for the presence of Alkaloids, Carbohydrates, Cardiac glycosides, Flavonoid, Phenols, Saponins, Tannins, Terpenoids, Quinones, and Proteins respectively.

1. Test for Flavonoids: 2 ml of each extract was added with few drops of 20% sodium hydroxide, the formation of intense yellow color is observed. To this, few drops of 70% dilute hydrochloric acid was added and yellow color was disappeared which indicates the presence of flavonoids in the sample extract.

2. Test for Alkaloids: To 1 ml of each extract, 1 ml of marquis reagent, 2ml of concentrated sulphuric acid and few drops of 40% formaldehyde were added and mixed, the appearance of dark orange or purple color indicates the presence of alkaloids.

3. Test for Saponins: To 2 ml of each extract, 6 ml of distilled water was added and shaken vigorously; formation of bubbles or persistent foam indicates the presence of Saponins.

4. Test for Tannins: To 2 ml of each extract, 10% of alcoholic ferric chloride was added; formation of brownish blue or black color indicates the presence of tannins.

5. Test for Phenols: To 2 ml of each extract, 2 ml of 5% aqueous ferric chloride was added; formation of a blue color indicates the presence of phenols in the sample extract.

6. Test for Proteins: To 2 ml of each extract, 1 ml of 40% sodium hydroxide and few drops of 1% copper sulfate was added; formation of violet color indicates the presence of peptide linkage molecules in the sample extract.

7. Test for Cardiac Glycosides: To 1 ml of each extract, 0.5ml of glacial acetic acid and 3 drops of 1% aqueous ferric chloride solution was added and formation of the brown ring at the interface indicates the presence of cardiac glycosides in the sample extract.

8. Test for Terpenoids: Take 1 ml of an extract of each solvent and add 0.5 ml of chloroform followed by a few drops of concentrated sulphuric acid, the formation of reddish-brown precipitate indicates the presence of Terpenoids in the extract.

9. Test for Carbohydrates: Take 1 ml of extract, add few drops of Molish reagent and then add 1 ml of concentrated sulphuric acid at the side of the tubes. The

mixture was then allowed to stand for 2 to 3 minutes. Formation of red or dull violet color indicates the presence of carbohydrates in the sample extract.

Preparation of Nanoparticles:

The Salt of (Ni $NO_3.6H_2O$) of 1 M solution dissolve in 100 ml of deionized water then slowly add 5 ml of plant extract to this solution.The dropwise addition of plant extracts to given metal solution and keep the solution for 3 hrs. During the reaction, the change in color of salt to the change in color of addition process will be observed.The final observation of color change will confirm the formation of nanoparticles. The synthesized nanoparticles centrifuge at 3000 rpm for 20-30 min. The supernatant was washed up to complete removal of an impurity present in it. Then the supernatant was decanted and nanoparticles were separated.

Instruments and techniques

Structural characteristics, crystallinity, and purity information were recorded by X-ray diffraction (XRD) patterns were recorded using a Rigaku Rotalflex RU-200B diffractometer with a CuKα (λ= 1.5418A°) in the scanning angle of 20 to 80 degrees. Surface morphological studies were performed by using a scanning electron microscope (FE-SEM) unit (S-4800 instrument from Hitachi, Japan) operated at 15.0 kV. Infrared spectroscopy (FT-IR) was measured on a Shimadzu FTIR-8400 FT-IR spectrometer 400 cm^{-1} to 4000 cm^{-1} at room temperature. The UV-Vis absorption study was performed at room temperature in the wavelength range of 200-800 nm on a UV-Vis spectrometer (Shimadzu UV-1700).

III. RESULTS AND DISCUSSIONS

Phytochemical screening:

Table 1. Phytochemicals analysis

Sr.no.	Phytochemicals test	Procedure	Present/Absent
1	Carbohydrates	Plant extract + 1-naphthol + Conc. Sulphuric acid	-
2	Protein	Plant extract + copper sulphate solution + KOH solution	+
3	Alkaloids	Plant extract + Meyers Reagent	_
4	Flavonoid	2 ml plant extract + ammonium hydroxide solution	+
5	Terpenoids	2ml plant extract+ Chloroform + Conc. sulphuric acid	+
6	Cardiac Glycosidase	2ml plant extract+ 3ml of Chloroform+ 10% ammonia solution	+
7	Tannins	Plant extract + few drops of lead acetate	+
8	Saponins	Plant extract + distilled water	-
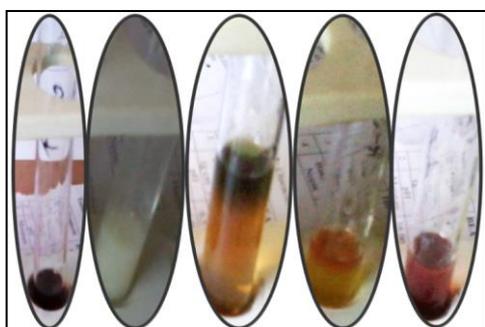
Figure 2. Phytochemicals present in B.monosperma

In this plant extract performing the various tests for phytochemical screening which indicates the presence of Proteins, Flavonoids, Terpenoids, Cardiac Glycosidase and Tannins etc. plays a more fundamental role in bio-based nanoparticles synthesis shown in Figure 2 and Table 1.
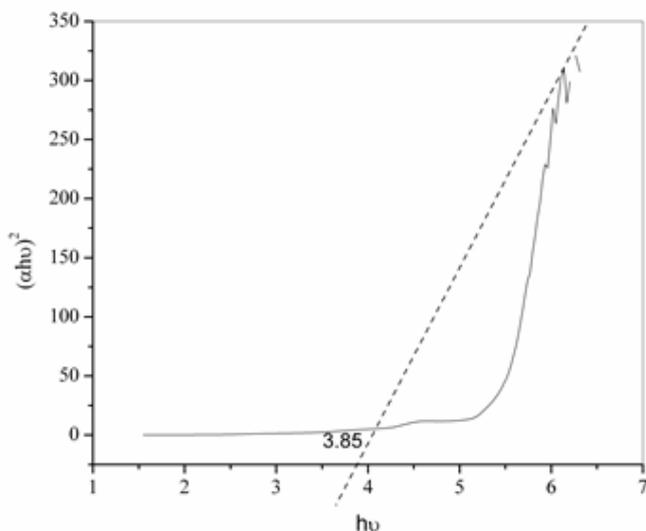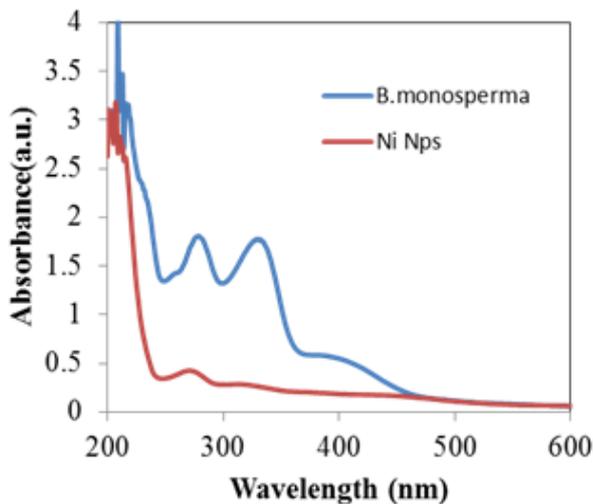
Figure 3. (a) UV-Visible Spectrum of Nickel nanoparticles (b) Band gap calculation

The color changes observed in metal solution after the B. monosperma extract addition and confirmation of nanoparticles was done by using UV-Visible spectroscopy (Figure 3 a). The UV-visible spectra imply that rapid bio-reduction takes place by using B. monosperma extract. In this study, we can conclude that the plant extract plays an important role in bio-reduction as well as stabilization of nanoparticles. The UV-visible absorption spectrum of the NiO particles obtained at room temperatures and dispersed in Water. The optical band gap energy of NiO nanoparticle produced at RT. A strong absorption peak at 285 nm is observed, attributable to the n to π^* transition of Ni-O bonds. The small absorption peak observed in the range 300-400 nm due to water present in (Ni $NO_3.6H_2O$) [18]. The *B. monosperma* extract shows two major peaks in 200-400 nm that is characteristic of flavonoid moiety [19, 20]. According to the data of the absorption spectra, the

optical band gaps (Eg) of NiO nanoparticles estimated by using the following equation:

$$(\alpha h\nu)^n = A (h\nu - E_g)$$

Where hν is photo energy, α is absorption coefficient, A is a constant relative to the material and n is either 2 for direct band gap material or 1/2 for an indirect band gap material. According to the equation, the optical band gap for the absorption peak obtained by extrapolating the linear portion of the $(\alpha h\nu)^n$ hν curve to zero. The increasing trends of the band gap energy upon the decreasing particles size is likely due to the defects or vacancies present in the intergranular regions generating new energy level to reduce the band gap energy [21].No linear relation was found for n = 1/2, suggesting that the as-synthesized NiO nanostructures are semiconducting with the direct transition at this energy [22].

The FT-IR spectrum of Nickel nanoparticles and B.monosperma:
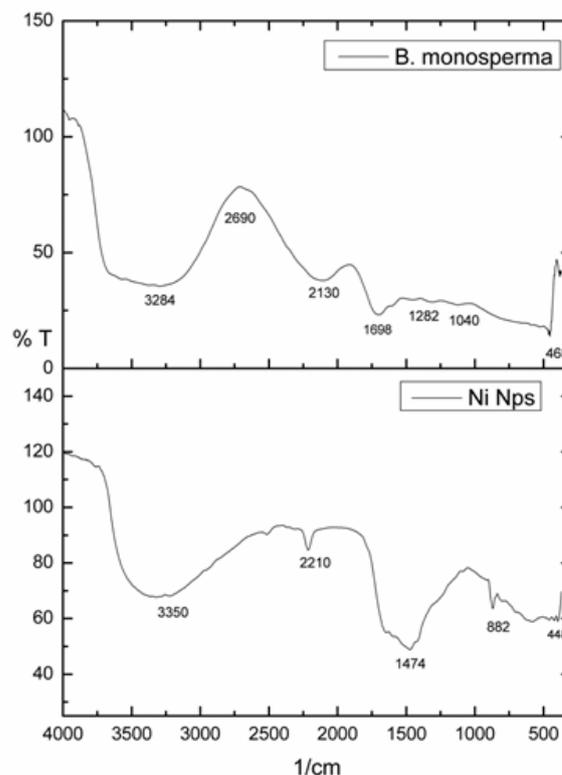
Figure 4. The FT-IR spectrum of Nickel nanoparticles and B.monosperma

In the FT-IR spectra of Butea monosperma flower extract Figure 4(a). the strong absorption peaks observed at 3284cm-1 (Hydrogen bonded OH Stretch), 2690 cm-1 (C-H Stretch in CH_2), 1698 cm-1 (C=C Symmetric Stretch), 1463.19 cm-1(C-H deformation in CH_2 and CH_3), 1282 cm-1(C-H Stretch), 1040 cm-1 (C-O Stretch of secondary alcohol), below 800 cm-1(=C-H bending exocyclic CH_2) [23]. The nickel nanoparticles

in Figure no.4 (b) intercalated hydroxyl group from water between 3100 and 3500 cm−1 [24, 25]. The 2210 cm-1 is revealed to -CN group frequency.Also, an H-O-H bend is observed at 1474 cm−1 from the vibration of free water molecules [24].The spectrum also shows a sharp O-H stretch at 882 cm−1 from the hydroxyl lattice vibration and a weak peak at 448 cm−1 indicating a Ni-O lattice vibration [25].

X-ray diffraction of Nickel Nanoparticles:
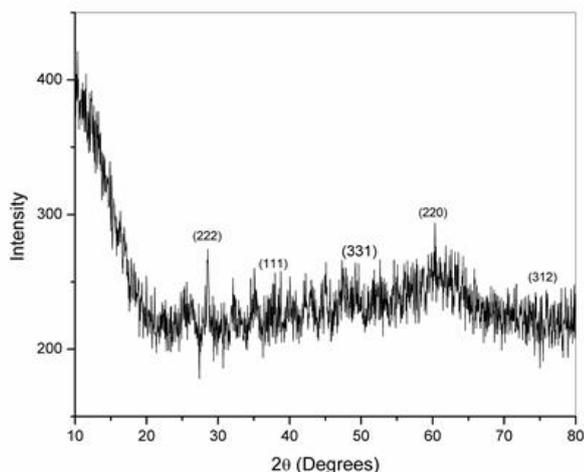
Figure 5. XRD spectrum of Nickel nanoparticles

XRD is used for the identification, purity, and quantitative analysis of NPs. The phase of NPs is determined by recording the peaks at 2θ value; these peaks give the value of crystal planes for a particular type of NPs [26]. In figure no.5 by comparing the position and intensity of these diffraction peaks with Joint Committee on Powder Diffraction Standard (JCPDS) card number (each)type of metal has specific JCPDS card number) one can identify the NPs and their phase (Cubic, spherical, wurtzite etc.).The intensity of XRD spectrum peaks is function of particle crystallinity. When the NPs have good crystallinity then intense and sharp peaks were observed and vice versa. The NPs size calculated using Scherrer equation; when the particle size is large then XRD patterns become broad:

$$D = \frac{0.98\lambda}{\beta Cos\theta} \qquad [1]$$

Where, is particle size, λ is wavelength (CuKα), β is FWHM, and θ is diffraction angle. The average particle size calculated by Debye-Scherrer formula was found to be 31.77 nm. In this study the X-ray diffraction study the scanning angle is 10° to 80 °.In this the, major peak values are mached 37.27 (222), 47.402 (331), 43.298 (200), 62.836 (220) and 75.437 (312) with JCPDS card no.89-5881 and 780643, which clears that Cubic size nanoparticles are synthesized. The d value obtain from the more intense peak is1.6250 which is in good

agreement with stanthe dard result of nickel nanoparticles.The inter planer distance (d) was calculated from Bragg's law,

$$2d \sin\theta = n\lambda \qquad [2]$$

Surface morphology:
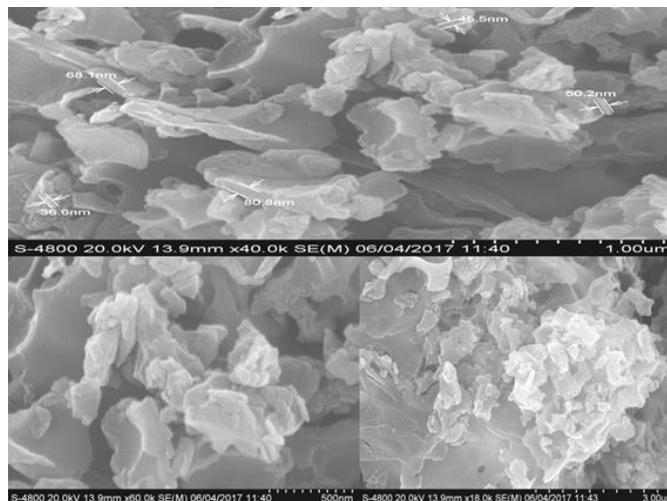
Figure 6. SEM image of Nickel nanoparticles

In Figure 6 the SEM is used to study morphology and composition of nanoparticles by scanning the surface with a high energy beam, produced by a heated filament.It is known that grain size and morphology of particles depends on reaction parameters such as temperature and gases generated (N_2, NO_2, CO_2, and H_2O).The aggregation occurs in nanoparticles because of magnetic interaction in nanoparticles[27].The results indicate that the nanoparticles were monocrystalline in nature and the average particle size was observed 56-60 nm.The flowers petal-like morphology observed in SEM images.The plant extract plays a crucial role in stabilizing as well as capping the nanoparticles.The aggregation observed in nickel nanoparticles and due to that some nanoclusters like morphology appeared.

XRD crystallinity index:
It was generally agreed that the peak breadth of a specific phase of the material is directly proportional to the mean crystallite size of that material. From our XRD data, a peak broadening of the nanoparticles was noticed. The average particle size, as determined using the Scherer equation, was calculated to be 31.77 nm. Crystallinity was evaluated through comparison of crystallite size ascertained by SEM particle size determination. Crystallinity index Equation is presented below:

$$Icry = \frac{D_P(SEM)}{D_{cry}(XRD)} \quad I_{cry} \geq 1 \qquad [3]$$

Where I_{cry} is the crystallinity index; Dp is the particle size (obtained from either TEM or SEM morphological analysis); Dcry is the particle size (calculated from the Scherrer equation).

Table 2. Crystallinity index of the sample

Sample	D_p(nm)	D_{Cry} (nm)	I_{Cry} (unitless)	Particle type
NiO	60	31.77	1.8885	Monocrystalline

Table.2. displays the crystallinity index of the sample that scored higher than 1.0. The data indicate that the NiO is crystalline. If the I_{cry} value is close to 1, then it is assumed that the crystallite size represents mono-crystalline whereas a polycrystalline have a much larger crystallinity index [28].

The SEM is used to study morphology and composition of nanoparticles by scanning the surface with a high energy beam, produced by a heated filament.The results indicate that the nanoparticles were monocrystalline in nature and the average particle size was observed 56-60 nm.The flowers petal-like morphology observed in SEM images.The plant extract plays a crucial role in stabilizing as well as capping the nanoparticles.The aggregation observed only on the surface of nickel nanoparticles but the pure nanoparticles show their own morphology and characteristics.

IV. CONCLUSION

The use of Butea monosperma extract is more useful than any other reductants because of faster bioreduction rate of production of nanoparticles.The green method of nanoparticle synthesis is simple, efficient, eco-friendly and did not require ample of reactants, draggy procedures and complex apparatus which were required for conventional methods.The *Butea monosperma* extract is more suitable for capping and stabilization of nickel nanoparticles.In this study, the formed nanoparticles show the band gap value of 3.85 eV which larger than bulk value 3.73 eV.The in-band gap value decreases particle size.i.e. formation of nanoparticles.These features help in the commercialization of Ni and NiO NPs in the fields of environmental cleaning and nanomedicine, electrical, optical devices.

V. Acknowledgments

VI. REFERENCES

[1]. N. R. Jana, Y. F. Chen, X. G. Peng, Size- and Shape-Controlled Magnetic (Cr, Mn, Fe, Co, Ni) Oxide Nanocrystals via a Simple and General Approach, Chemistry of Materials, 16(2004) 3931-3935.

[2]. W.Wei, X. Jiang, L. Lu, X. Yang, X. Wang, Study on the catalytic effect of NiO nanoparticles on the thermal decomposition of TEGDN/NC propellant, Journal of Hazardous Materials,168(2009) 838-842.

[3]. W. Wang, Y. Liu, C. Xu, C. Zheng, G. Wang, Synthesis of NiO nanorods by a novel simple precursor thermal decomposition approach, Chemical Physics Letters, 362 (2002) 119-122.

[4]. N.M. Hosny, Synthesis, characterization and optical band gap of NiO nanoparticles derived from anthranilic acid precursors via a thermal decomposition route, Polyhedron, 30 (2011) 470-476.

[5]. X. Li, X. Zhang, Z. Li, Y. Qian, Synthesis and characteristics of NiO nanoparticles by thermal decomposition of nickel dimethylglyoximate rods, Solid State Communications,137 (2006) 581-584.

[6]. L. Xiang, X.Y. Deng, Y. Jin, Experimental study on the synthesis of NiO nano-particles, Scripta Materialia, 47 (2002) 219-224.

[7]. Y. Wang, J.-J. Ke, Preparation of nickel oxide powder by decomposition of basic nickel carbonate in microwave field with nickel oxide seed as a microwave absorbing additive, Materials Research Bulletin, 31 (1996) 55-61.

[8]. K. Anandan, V. Rajendran, Morphological and size effects of NiO nanoparticles via solvothermal process and their optical properties, Materials Science in Semiconductor Processing, 14 (2011) 43-47.

[9]. Z. Wei, H. Qiao, H. Yang, C. Zhang, X. Yan, Characterization of NiO nanoparticles by anodic arc plasma method, Journal of Alloys and Compounds, 479 (2009) 855-858.

[10]. S. Mohseni Meybodi, S.A. Hosseini, M. Rezaee, S.K. Sadrnezhaad, D. Mohammadyani, Synthesis of Wide Bandgap Nanocrystalline NiO Powder

via a Sonochemical Method, Ultrasonics Sonochemistry, 19 (2012) 841-845.

[11]. X.Deng, Z. Chen, Preparation of nano-NiO by ammonia precipitation and reaction in solution and competitive balance, Materials Letters, 58 (2004) 276-280.

[12]. Y. Du, W. Wang, X. Li, J. Zhao, J. Ma, Y. Liu, G. Lu, Preparation of NiO nanoparticles in microemulsion and its gas sensing performance, Materials Letters, 68 (2012) 168-170.

[13]. R. C. Monica, R. Cremonini, Nanoparticles, and higher plants, Caryologia, 62(2009) 161-165.

[14]. A. Ahmad, P. Mukherjee, S. Senapati et al., Extracellular biosynthesis of silver nanoparticles using the fungus Fusarium oxy sporum, Colloids, and Surfaces B: Biointerfaces, 28(2003)313-318.

[15]. S.J.Kulkarni, Synthesis of Silver nanoparticles from the plant and fruit extracts-summary on research and studies, International Journal of Scientific Research in Chemistry, 2(2017)16-21.

[16]. F. T. Thema, E. Manikandan, A. Gurib-Fakim, M. Maaza, Single phase Bunsenite NiO nanoparticles green synthesis by Agathosma betulina natural extract, Journal of Alloys and Compounds, 657(2016) 655-661.

[17]. M. Singh, S.Manikandan, A. Kumaraguru, Nanoparticles: a new technology with wide applications, Research Journal of Nanoscience and Nanotechnology, 1(2011) 1-11.

[18]. M. A. Nasseri, F. Ahrari, B. Zakerinasab, A green biosynthesis of NiO nanoparticles using an aqueous extract of Tamarix serotina and their characterization and application, Applied Organometallic Chemistry, 30 (2016) 978-984.

[19]. J. B. Harborne, Phytochemical methods: Guide to modern techniques of plant analysis, 3rd ed. Springer, India (1973) 60-79.

[20]. Tun, A. A., A. M. Hlaing, H. P. Aung, M. M. Htay., Isolation and characterization of flavonoids from the flowers of Butea monosperma Lam (Pauk), Journal of the Myanmar Academy of Arts and Science. 2 (2004) 85-90.

[21]. F.F.Lange, Powder processing science, and technology for increased reliability, Journal of the American Ceramic Society, 72 (1989) 3-15.

[22]. S.S. Hwang, A.L. Vasiliev, N.P. Padture, Improved processing and oxidation-resistance of ZrB2 ultra-high temperature ceramics containing SiC nano dispersoids, Materials Science and Engineering: A, 464 (2007) 216-224.

[23]. M. K. Das, P. M. Mazumder, S. Das, Antiepileptic Activity of Methanol Extract of Butea monosperma (Lam.) Kuntze and its Isolated Bioactive Compound in Experimentally Induced Convulsion in Swiss Albino Mice, International Journal of Drug Development and Research 8(2016) 1.

[24]. K. Harish, R. Renu, S. R. Kumar, Synthesis of nickel hydroxide nanoparticles by reverse micelle method and its antimicrobial activity, Research Journal of Chemical Sciences, 1(2011) 42-48.

[25]. Q. Song, Z. Tang, H. Guo, S. L. I. Chan, Structural characteristics of nickel hydroxide synthesized by a chemical precipitation route under different pH values, Journal of Power Sources, 112 (2002) 428-434.

[26]. B.T. Sone, X.G. Fuku, M. Maaza, Physical and Electrochemical Properties of Green Synthesized Bunsenite NiO Nanoparticles via Callistemon Viminalis' Extracts, International Journal of Electrochemical Science,11 (2016) 8204 - 8220.

[27]. R. A. Raj, M. S. AlSalhi, S. Devanesan, Microwave-Assisted Synthesis of Nickel Oxide Nanoparticles Using Coriandrum sativum Leaf Extract and Their Structural-Magnetic Catalytic Properties, Materials 10 (2017) 460.

[28]. P. Xubin, M. R. Iliana, M. Ray, L. Jingbo, Nanocharacterization and bactericidal performance of silver modified Titania photocatalysts, Colloids and Surfaces B: Biointerfaces. 77(2010)82-89.